ACS APPLIED MATERIALS & INTERFACES

Research Article

www.acsami.org

Bioinspired Plate-Based Fog Collectors

Xin Heng and Cheng Luo*

Department of Mechanical and Aerospace Engineering, University of Texas at Arlington, 500 W. First Street, Woolf Hall 226, Arlington, Texas 76019, United States

Supporting Information

ABSTRACT: In a recent work, we explored the feeding mechanism of a shorebird to transport liquid drops by repeatedly opening and closing its beak. In this work, we apply the corresponding results to develop a new artificial fog collector. The collector includes two nonparallel plates. It has three advantages in comparison with existing artificial collectors: (i) easy fabrication, (ii) simple design to scale up, and (iii) active transport of condensed water drops. Two collectors have been built. A small one with dimensions of 4.2 × 2.1 × 0.05 cm^3 (length × width × thickness) was first built and tested to examine (i) the time evolution of condensed drop sizes and (ii) the collection processes and efficiencies on the glass, SiO_2, and SU-8 plates. Under similar experimental conditions, the amount of water collected per unit area on the small collector is about 9.0, 4.7, and 3.7 times, respectively, as much as the ones reported for beetles, grasses, and metal wires, and the total amount of water collected is around 33, 18, and 15 times. On the basis of the understanding gained from the tests on the small collector, a large collector with dimensions of 26 × 10 × 0.2 cm^3 was further built and tested, which was capable of collecting 15.8 mL of water during a period of 36 min. The amount of water collected, when it is scaled from 36 to 120 min, is about 878, 479, or 405 times more than what was collected by individual beetles, grasses, or metal wires.

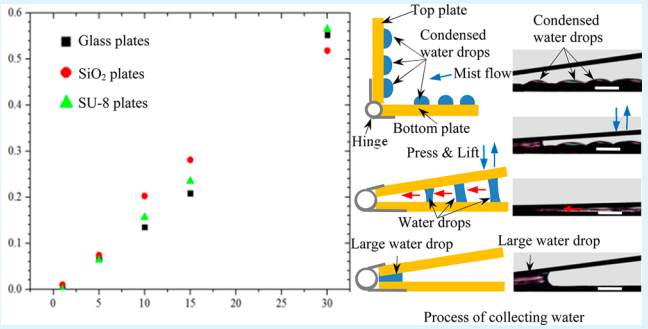

KEYWORDS: *water collector, squeezing and relaxing, fog, shorebird*

1. INTRODUCTION

Deserts roughly cover about one-quarter of the Earth's land area, and semideserts cover another quarter.[1] They have little rainfall every year. Fog and dew in some deserts may deliver more water than rainfall[1] and may be important water sources, e.g., to beetles,[2,3] cacti,[4,5] *cotula fallax plants*,[6] and dune grasses *Stipagrostis subulicola*.[7,8] What these species use to collect water from fog and dew in a desert obviously provides a new insight into obtaining water. As commented in ref 6, for the purpose of collection, a special controlling mechanism is needed to guide the movements of condensed water drops. Otherwise, these drops would be quickly lost to the heat and winds of the desert. Thus, water collection is not as simple as it may seem.[6]

Both capillary and gravitational forces have been employed in animals and plants to guide the movements of condensed drops through their specific surface structures. It is reported that a beetle living in the Namib Desert can collect water from fog and dew through microbumps on its back. The peaks of these microbumps are hydrophilic, whereas the troughs are superhydrophobic.[2] The water in the fog forms fast-growing drops on these peaks. As a drop reaches a size of 4−5 mm in diameter, the gravity of the drop overcomes the capillary force that makes it attach to the peak, and the drop rolls down the beetle's surface to the mouth part.[2] It is also reported that cacti can harvest water from the fog and dew using the spines distributed on its surface.[4,5] Microbarbs are grown on a spine, forming a hierarchical wire structure. The spine and microbarb have lengths with the orders of 1 mm and 10 μm, respectively. Both spines and microbarbs have conical shapes, whose diameters gradually increase from the tip to the root of a wire. A water drop that is condensed, e.g., on the tip of the spine or the microbarb can be driven to the root by a capillary force induced by this diameter gradient.[9] With the aid of gravity, the large drop on the spine root is sucked into the underneath cluster. A similar mechanism has been used to collect fog in the cases of *Cotula fallax* plants, dune grasses *Stipagrostis subulicola*, and spiders. That is, hierarchical structures are used as the condensation spots of water vapors due to the large surface area, and the condensed drops are subsequently transported to desired locations due to capillary and gravitational forces. In the case of *Cotula fallax* plants, the leaves and the fine hairs on the leaves form hierarchical structures.[6] Water drops are first condensed on the leaves. When the drops become too large to be supported by the leaves, they fall to the roots, which spread over 20 m like a carpet. A similar approach is also used by the dune grasses *Stipagrostis subulicola* to collect fog.[7,8] As for a spider, its silk is periodically covered by puffs (made of nanofibers) and joints,[10] which form spindle-knots when contacting water vapors. Because of a capillary force generated by the conical shape

Received: July 8, 2014
Accepted: August 25, 2014
Published: August 25, 2014

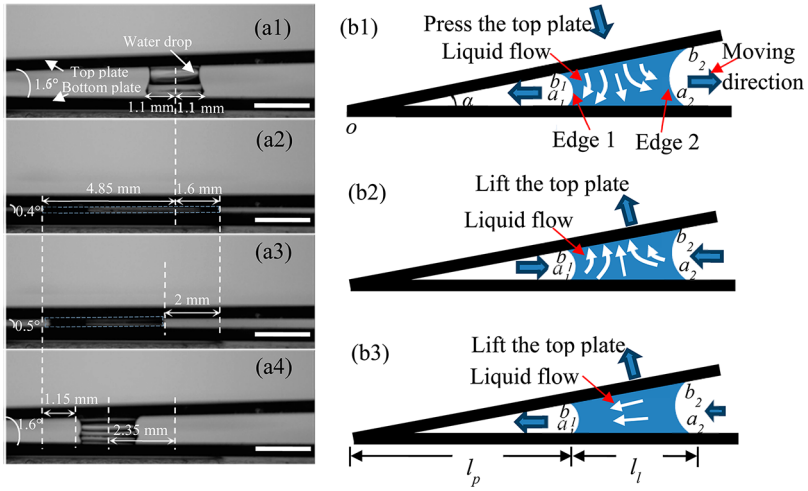

Figure 1. (a) Experimental results of squeezing and relaxing processes using two SiO_2 plates: (a1) squeezing of the drop, (a2) squeezed drop, (a3) relaxing of the drop, and (a4) relaxed drop. Scale bars in (a) represent 2 mm. (b) Cross-sectional schematics of flow patterns and edge movements of a lyophilic liquid drop during (b1) squeezing and (b2, b3) relaxing processes.

and different roughnesses of the silk surface, water drops can be guided to specific locations on the silk and are expected to also fall down when they become too heavy to be supported by the silk.

Several artificial fog collectors have been developed. They mimicked the fog-collection mechanisms of beetles and used micropeaks to collect fog.[2,11−15] On the other hand, it is considered that a hierarchical wire structure, as in the cases of cacti, *Cotula fallax* plants, dune grasses, and spider silk, should have higher fog-collection efficiency than micropeaks, because the hierarchical wire structure has a much larger surface area. As a matter of fact, the collection efficiency of a desert beetle has been compared with that of dune grasses *Stipagrostis subulicola*.[8] It was found that dune grasses were more efficient in harvesting fog during the same time period of 120 min in terms of both totally collected water and harvested water per unit area. It is also noted that conical-shaped copper wires have been tested in the research laboratories for fog collection.[16] In addition, mesh nets are also used to harvest fog.[17] A net consists of two families of intertwined fibers. Accordingly, it is a linewise structure with each fiber visualized as a line. The fog that goes through the net holes cannot be harvested. Furthermore, vertically oriented plates with hydrophilic or hydrophobic surfaces have been used to collect fog.[18,19] Due to gravity, large drops that are condensed on a plate can be drained to the container, which is located under the plate. On the other hand, tiny drops may still stick to the plate, since they may not be heavy enough to overcome the constraint of surface tension.

Various hierarchical wire structures, such as branched ZnO nanowire structures,[20−26] have been recently synthesized. Their large surface areas make them have potential applications in, for instance, solar energy conversion.[26,27] However, the lengths of the structures are normally in the microscale, and the branched wires are in the nanoscale. In contrast, the hierarchical wire structures of plants have at least millimeter-scaled lengths. Accordingly, we have recently developed branched ZnO wire structures, whose sizes are comparable to or larger than the spine structures of the cacti.[5] They have been successfully applied to collect water. In addition, other researchers also reported continuous collection of fog employing (i) conical microtip arrays, which have cactus spine-like shapes, and (ii) the hydrophilic cotton matrix.[28]

Because it involves much effort to fabricate large branched wire structures, in this work, we desire to develop a new collector, which uses two large plates to collect water from fog. The development of such a collector is motivated by the feeding mechanism of a shorebird. It has been reported that some feeding shorebirds with long thin beaks, such as phalaropes, are capable of driving liquid drops to move toward their mouths by opening and closing the beaks.[29−33] The drop movement is to transport the prey that may be contained in a liquid drop. This feeding process provides a new approach to control the movement of a water drop. As will be detailed in section 3, the adoption of this method to develop an artificial collector results in three advantages in comparison with existing artificial collectors. First, unlike the mesh nets, the plates have much larger condensation areas, and the condensation water is actively transported to the desired locations. Thus, collection efficiency is improved. Second, it does not involve any hierarchical wire structures, which reduces the fabrication effort. Third and finally, because the manufacturing of plates is simple, it is easy to scale up the device to collect more water by using large plates.

2. TRANSPORTATION MECHANISM AND MOTIVATION

Squeezing and relaxing processes are used in the shorebirds to guide the drop movement.[29−33] Their physical mechanisms have been explored for the case when the trailing and leading edges of the drop are pinned, respectively, during the squeezing and relaxing processes.[33,34] In a recent work, we have further explored the situation when both edges are not pinned during those processes.[35] Figure 1 gives a typical cycle of squeezing and relaxing processes that a shorebird uses to guide the unidirectional movement of a water drop. The corresponding demonstration is through an artificial beak that we developed. This artificial beak includes two nonparallel SiO_2-coated Si plates, which play a role similar to the shorebird beak. In the squeezing process (Figure 1a1 and a2), the water drop is pressed by the top plate into a pancake-like shape. In the relaxing process (Figure 1a3 and a4), the top plate is lifted up and the left edge of the drop may slightly move rightward, while the right edge has a relatively large leftward displacement. As a result, the whole drop is shifted toward the corner of the two

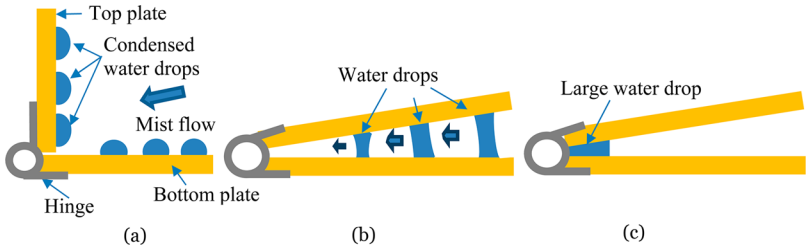

Figure 2. Process of collecting water: (a) open the two plates to collect fog; (b) squeeze and relax condensed water drops to drive them toward the channel located at the end of the bottom plate, and (c) after water drops stay in the corner, pump them away through the channel.

plates at the end of the relaxing process. Repetition of these two processes results in the continuous movement of the drop toward the corner.

This shifting is caused by different pressure distributions inside the drop during the squeezing and relaxing processes. As illustrated in Figure 1b1, for simplicity, the left and right edges of the liquid drop are called "Edge 1" and "Edge 2", respectively. We use o and α, respectively, to denote apex edge and opening angle of the two plates. Let a_1 and b_1 denote the two points where Edge 1 intersects with the bottom and top plates, separately, and set a_2 and b_2 to be the two intersecting points that Edge 2 forms with the bottom and top plates, respectively.

When the liquid drop is pressed, the liquid pressure at b_1b_2, which is the interface between the drop top and the top plate, is increased. This pressure is now higher than those at Edge 1, Edge 2, and a_1a_2. Hence, as illustrated in Figure 1b1, the liquid is driven by the pressure difference to flow toward these edges, making Edges 1 and 2 move left- and rightwards, respectively. When the liquid drop is relaxed by lifting the top plate, the liquid pressure at b_1b_2 is reduced. This pressure is now lower than those at Edge 1, Edge 2, and a_1a_2. As illustrated in Figure 1b2, the liquid is driven by the pressure difference to flow away from these edges, making Edges 1 and 2 move right- and leftwards, respectively.

Let p_{w1} and p_{w2} represent liquid pressures at Edges 1 and 2, respectively. The critical difference between the squeezing and relaxing processes is that, in the squeezing process, even if there exists a difference between p_{w1} and p_{w2}, this difference does not cause a horizontal flow inside the drop, because the pressure in the middle of the drop, p_{wm}, is larger than both p_{w1} and p_{w2}. As illustrated in Figure 1b2, $(p_{wm} - p_{w1})$ and $(p_{wm} - p_{w2})$ make liquid move left- and rightwards, respectively. However, in the relaxing process, p_{wm} is less than both p_{w1} and p_{w2}. Hence, in addition to the flow patterns illustrated in Figure 1b2, liquid between Edges 1 and 2 can also be pushed to flow leftwards by $(p_{w2} - p_{w1})$ (Figure 1b3), which has the following expression:[35]

$$p_{w2} - p_{w1} = \frac{\gamma \cos \theta_r}{\sin \frac{\alpha}{2}} \left(\frac{1}{l_p} - \frac{1}{l_p + l_l} \right) \quad (1)$$

where l_p denotes the distance between o and a_1, l_l is the length of a_1a_2, and θ_r denotes the receding contact angle. Accompanied with this flow, Edge 2 may also move leftwards. The combination of the two situations shown in Figure 1b2 and b3 indicates that the rightward movement of Edge 1 is reduced or stopped, while the leftward movement of Edge 2 may be enhanced. Accordingly, the drop is shifted leftward at the end of the relaxing process in comparison with the corresponding position at the beginning of the squeezing.

In terms of the movements of Edges 1 and 2, the relaxing is not a reversible process of the squeezing. On the other hand, if the two plates are parallel, i.e., $\alpha = 0°$, then, due to geometric symmetry, we have $p_{w2} = p_{w1}$. Accordingly, the flow pattern shown in Figure 1b3 does not exist. Thus, the relaxing is a reversible process of the squeezing, and there is no shifting effect, as previously observed in experiments.[36−39]

When water drops, which have condensed on plate surfaces, are squeezed between two plates, they should spread and merge together to form a large drop. By eq 1, it is readily shown that, for fixed α and l_p, $(p_{w2} - p_{w1})$ increases with the increase in l_l. Accordingly, the leftward movements of both Edges 1 and 2 that are illustrated in Figure 1b3 should also increase with the increase in l_l. This result indicates that the shifting effect increases with the size of the liquid drop. Thus, in comparison with individual condensed drops, the large drop formed by a group of them can be more easily transported to the plate corner, which provides a new approach to collect fog and further motivates us to develop a fog collector based on this approach.

3. DESIGN OF COLLECTORS AND EXPERIMENTAL SETUP

3.1. Design Criteria. The new fog collector has a shape similar to the beak of a shorebird. It includes two large nonparallel plates (Figure 2a). The collector is applied to collect fog through a two-step procedure. In the first step (Figure 2a), the two plates are opened at a relatively large angle, facing the incoming fog flow. After condensed water drops grow to a certain size, the top plate is lowered down, and the water drops are subsequently driven toward the corner of the two plates through squeezing and relaxing processes (Figure 2b), which is the second step. After a certain amount of water is accumulated in the corner, it is pumped away from the corner to start the next round of fog collection (Figure 2c).

The major concern about a fog collector is its collection efficiency. The amount of water that is collected per unit time by our plate-based collector should increase with the increase in the following two aspects: the amount of water vapor that is condensed on the two plates and the percentage of condensed water that can be transported to the corner of the two plates. The demand in the first aspect results in three design criteria: (i) the top plate should be oriented vertically to make its surface directly exposed to the mist flow; (ii) the bottom plate should be placed horizontally to avoid the loss of water drops due to gravity; and (iii) the plates should be as large as possible to have more surface area for water condensation. According to the first two criteria, the plate-based collector is designed as shown in Figure 2a. The selection of proper plate sizes for collectors based on the third criterion will be detailed in the next subsection.

The consideration of the second aspect yields two actuation criteria: (a) both small and large condensed drops should be transported to the corner of the two plates and (b) to simplify the operation, a water drop should be translated as far as possible during each cycle of squeezing and relaxing to reduce the number of actuation cycles. These two actuation criteria have been employed in this work to determine the condensation period.

3.2. Plate Sizes. Let l_1 and l_2 denote the dimensions of a plate, respectively, along the directions perpendicular and parallel to the intersecting line of the two plates. As will be justified later, the values of both l_1 and l_2 depend on the sizes of the condensed drops.

Let α denote the relaxing angle that is needed to translate a water drop during a relaxing process, and set h to denote the maximum height that a water drop can have before it breaks during the separation of the two plates. It is considered that $l_1 \gg h$. According to simple geometric analysis, the value of l_1 is related to α and h by

$$l_1 \leq \frac{h}{\alpha} \tag{2}$$

Obviously, h increases with the increase in the drop size. Also, it has been demonstrated that the translation of a liquid drop per actuation cycle increases with the increase in the drop size.[35] Thus, large condensed drops are desired to have a large value of l_1.

In principle, the value of l_2 can be as large as possible. In reality, it is limited by fabrication and assembly errors. These errors may create a gap between the two plates when these plates are put together. Accordingly, if the height of a water drop is smaller than the gap, then a water bridge could not be formed between the two plates to transport the drop. Hence, large condensed drops are also desired to have a large value of l_2. On the other hand, in a very dry environment, in which only small water drops may exist, the values of l_1 and l_2 should be reduced accordingly to ensure that water bridges could be formed between two plates to transport the corresponding water drops.

When the radius of a condensed water drop exceeds the capillary length of water, which is 2.7 mm, gravitational effect dominates. According to ref 40, the height of such a large drop is

$$e = 2l \sin\left(\frac{\theta}{2}\right) \tag{3}$$

where l denotes the capillary length of water and θ is the apparent contact angle of the water drop. e is also the maximum height that a water drop may have. Hence, the fabrication and assembly errors of the two plates should be less than e. Also, we should wait until the condensed drop has a radius larger than 2.7 mm before the start of the collection step. Once the height reaches the value of e, the continuous condensation does not increase the height of the drop, while it should increase the lateral dimension of the drop.

There exist three basic stages of condensation:[41,42] initial, intermediate, and large-drop formation. In these three stages, the average drop radii, R, are related to time, t, as $R \approx t^{1/3}$, $R \approx t$, and $R \approx t^{1/2}$, respectively. Thus, drops grow in a fast manner in the second stage, and the growth is slowed down in the third stage. Accordingly, the best timing to start the collection step is at the beginning of the third stage. On the other hand, the observation of the results in refs 41 and 42 indicates that the time duration of each stage depends on the substrate geometry, substrate coatings, and the incoming fog flow. These factors are experimentally examined in this work.

In addition, according to eq 3, e increases with the increase in θ. This implies that a more hydrophobic surface will result in a high value of e. On the other hand, a water drop actually moves away from the corner of the two plates in the hydrophobic case (i.e., $\theta > 90°$). In contrast, when θ is close to 0°, the drop may move toward the corner of the plates by itself without any actuation.[33,35] This implies that, for the transporting purpose, more hydrophilic surfaces are desired. Accordingly, a contradiction occurs regarding the value of θ. To find an optimal value of θ in terms of both the plate sizes and collection efficiency, we test glass plates, SiO_2-coated Si plates, and SU-8-covered glass plates. The corresponding values of θ on these plates are 18 ± 2°, 42 ± 2°, and 82 ± 2°, respectively. For simplicity, the latter two plates are called "SiO_2 plate" and "SU-8 plate", respectively. The three types of plates have rectangular shapes with the approximately same dimensions of 4.2 × 2.1 × 0.05 cm^3 (length × width × thickness).

3.3. Experimental Setup for a Small Collector. Two collectors have been built. A small one was first built and tested. As shown in Figure 3, the small collector included two identical

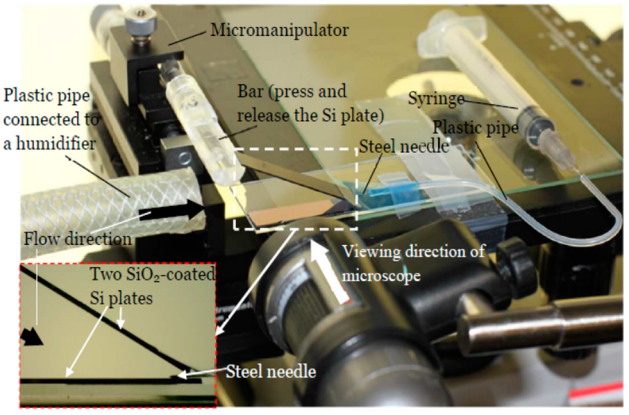

Figure 3. Experimental setup for water collection.

plates. The top plate was lifted or lowered down using a micromanipulator. At room temperature (22 ± 1 °C), a humidifier (model EE-5301, Crane USA Co.) was employed to generate a mist flow (Figure 3). A plastic tube was used to guide this mist flow. The tube had a diameter of 2 cm. It was comparable to the width of a plate. The relative humidity was 100% in the tested area. In the designed case (Figure 2a), the mist flow has a large incident angle on the top plate. However, the small collector was used to examine the minimum amount of vapors that might be condensed on a plate. It was expected that this would occur when the mist flow was parallel to this plate. Thus, in the small collector, the mist flow that came out of the tube was approximately along the horizontal direction and formed an angle of 15° with the bottom plate. The flow fully covered the bottom plate, while it had much less contact with the top plate.

The humidifier had been turned on for 1 min to ensure that the flow rate had been steady before the flow was pointed to the bottom plate, followed by the recording of the condensation and collection processes through an optical microscope. A steel needle was inserted at the corner of the two

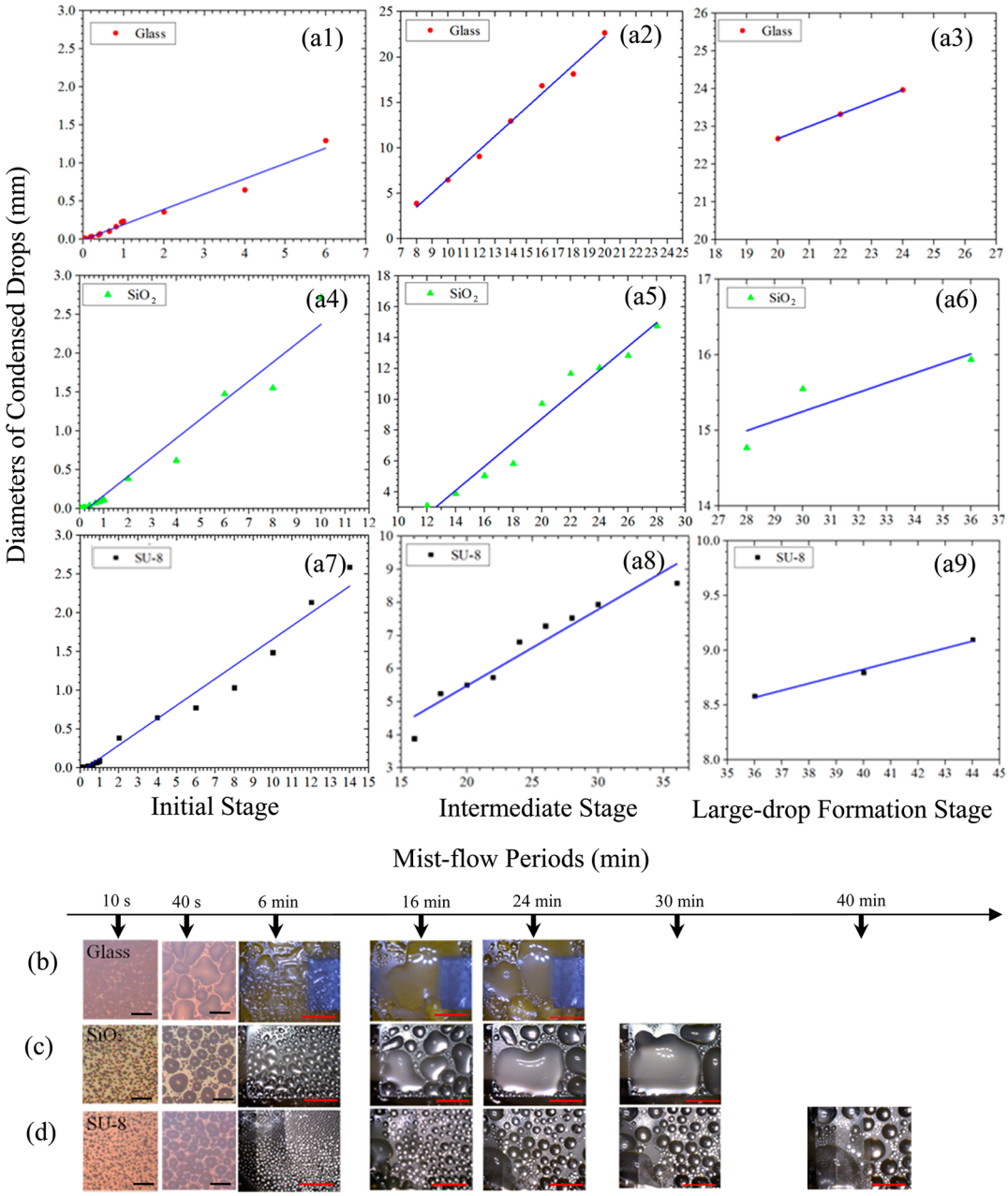

Figure 4. (a) Time evolution of diameters of condensed drops on the different plates, respectively, after 1−45 min. (b−d) Water drops on the glass, SiO_2, and SU-8 plates, respectively, after 10 s, 40 s, 6, 16, 24, 30, and 40 min condensation periods, respectively. Black and red scale bars represent 100 μm and 10 mm, respectively.

plates to collect water accumulated over there with the aid of a syringe that was connected to the needle. Tests were done on the three types of plates to find (i) the relation of the drop sizes with the condensation times, (ii) the number of actuation cycles needed to completely transport condensed drops from the plates to their corner, and (iii) the values of α and l_1. On the basis of the understanding gained on these tests, a large collector was subsequently designed and built to collect a large amount of water. The design and setup of the large collector will be detailed in subsection 4.3.

4. EXPERIMENTAL RESULTS AND DISCUSSIONS

4.1. Condensation. Figure 4 shows the time evolution of average diameters of condensed water drops after the bottom plate has been exposed to the mist flow from 0 to 45 min. After 8, 14, and 16 min, the radii of the condensed drops on glass, SiO_2, and SU-8 plates, respectively, have exceeded the capillary length of water. According to the relationship of the drop sizes with time, we divide the condensation process on each type of plate into three stages: initial, intermediate, and large-drop formation. The average radius of the drop is below the capillary length of water in the initial stage, while it is above it in the other two stages. However, the time durations and drop growth rates in these three stages vary with the type of plate. Different from what was reported in refs 41 and 42, except for the intermediate stage, the drop sizes in the other two stages also increased approximately linearly with time. On the other hand, as reported in refs 41 and 42, the drop growth rate was the largest in the intermediate stage.

Some phenomena observed on each type of plate are described below. For the glass plates, in the initial stage ($t \leq 8$ min, Figure 4a1), drops nucleated and tiny drops appeared and were densely distributed on the plate (Figure 4b). In the intermediate stage (8 min < t < 20

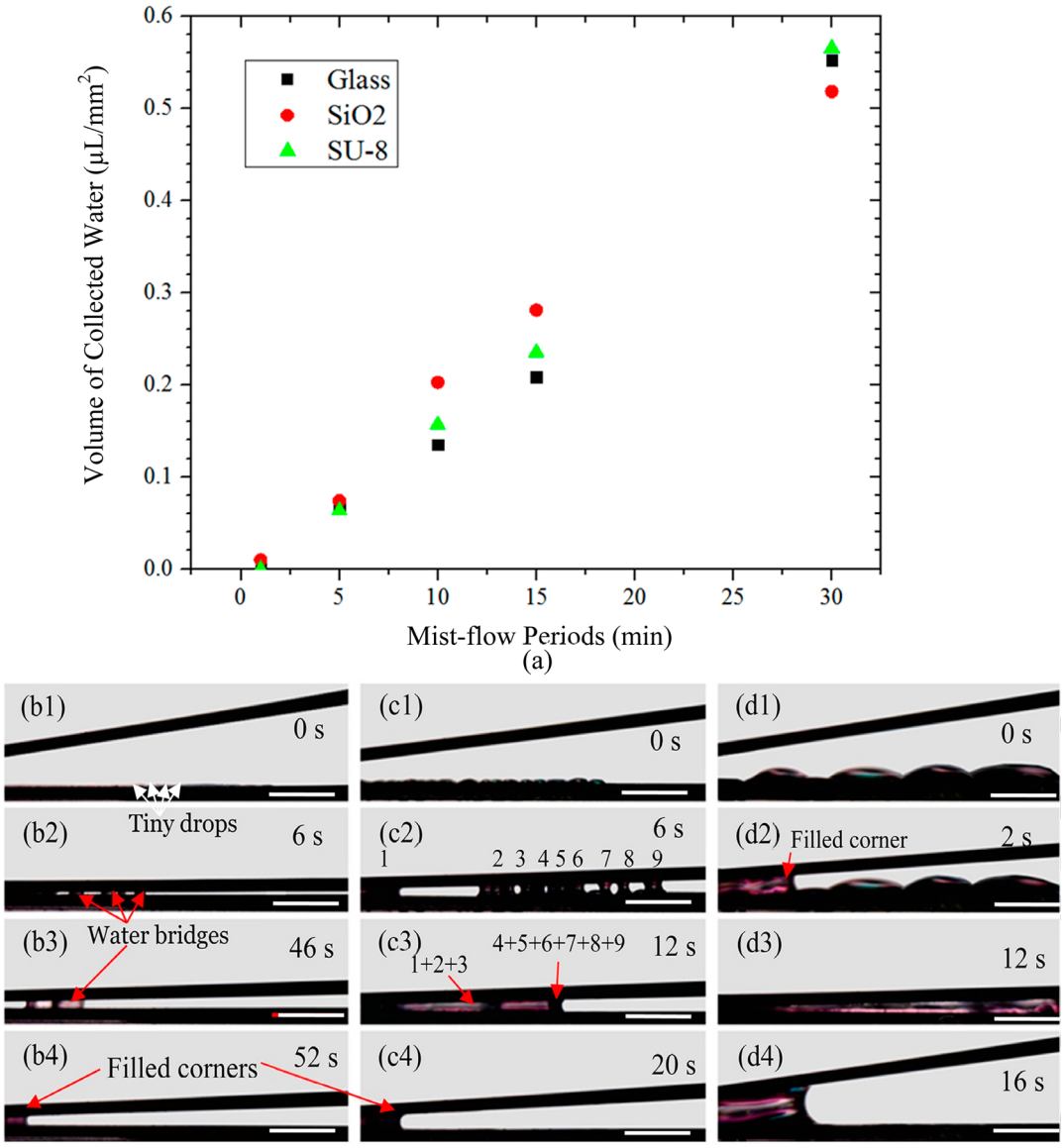

Figure 5. (a) Volumes of collected water per mm^2 corresponding to different mist-flow periods. Squeezing and relaxing of water drops after mist flows using SiO_2 plates for (b) 1, (c) 5, and (d) 30 min, respectively. (b1), (c1), and (d1), before the top plate is lowered down; (b2), (c2), and (d2), press the drops; (b3), (c3), and (d3), relax the drops; and (b4), (c4), and (d4), after 1 or more cycles, the corner of two plates is filled with water. Numbers in (c2) and (c3) represent different water drops, and "1 + 2 + 3", for example, means that drops 1, 2, and 3 are merged into one drop. Scale bars in (b–d) represent 2 mm. The corresponding videos of (b–d) are provided in Supporting Information.

min, Figure 4a2 and b), drops gradually increased their sizes with a higher rate of 1.6 mm/min than the one in the first stage (0.2 mm/min) due to coalescence of and condensation on pre-existing drops. In the stage of large-drop formation ($t \geq 20$ min, Figure 4a3), drops had diameters as large as 24.0 mm after 24 min, and tiny drops were also seen between the large ones (Figure 4b). In this stage, the growth rate of condensed drops decreased to 0.3 mm/min. When the glass plate was exposed to the mist flow for >30 min, the sizes of some drops were even beyond the width of the plate. Correspondingly, these drops spilled out of the plate.

Two different phenomena were observed on the SiO_2 plates in the initial ($t < 14$ min, Figure 4a4), intermediate (14 min $< t <$ 28 min, Figure 4a5), and large-drop formation ($t \geq 28$ min, Figure 4a6) stages. When the bottom SiO_2 plate was exposed to the mist flow for 30 min, the condensed drop reached the edge of the plate but did not spill out of the plate due to the relatively larger contact angle than the glass plate (Figure 4c). The fastest growth rate of condensed drop, which occurred in the intermediate stage, was 0.78 mm/min, which was about half of its counterpart in the case of glass plates. Drops had diameters as large as 15.9 mm after 36 min.

The condensation process on the SU-8 plates has both longer initial and intermediate stages ($t \leq 16$ min and 16 min $< t <$ 36 min, respectively, Figure 4a7 and a8) than those on glass and SiO_2 plates. In the stage of large-drop formation ($t \geq 36$ min, Figure 4a9), drops had diameters as large as 8.6 mm after 36 min, and tiny drops were also seen between the large ones (Figure 4d). The fastest growth rate of condensed drop, which occurred in the intermediate stage, was 0.2 mm/min, which was about one-third of its counterpart in the case of SiO_2 plates.

The differences among the phenomena on the three types of plates are considered to be induced by the different contact angles on the plates. When the plate surface is more hydrophilic, the condensed drops are easy to spread on this surface, making their diameters increase at a higher rate. Accordingly, on the glass plates, the initial and intermediate stages last the shortest periods, while their drops have the smallest heights in the large-drop formation stage.

4.2. Transport of Condensed Drops. For each type of plate, water was collected five times when condensation lasted 1, 5, 10, 15, and 30 min, respectively, under the same experimental conditions as discussed in subsection 4.1. Four tests were done each time, and the average value is given in Figure 5a. For easily identifying data, the error bars were not added to this figure. Instead, the errors are provided when the corresponding data are indicated in the following text. As indicated in subsection 3.2, the best time to start the transport of the condensed water drops is still at the beginning of the stage of large-drop formation. This stage starts at t = 20, 28, or 36 min on glass, SiO_2, or SU-8 plates. Given that water began to spill out of the glass plates at t = 30 min, the longest condensation period was chosen to be 30 min in our tests on the small collector.

Three interesting points were observed from Figure 5a. First, the collected water for each type of plate has an approximately linear relationship with the condensation time. This is considered reasonable, because in our tests the incoming mist flow is steady. Accordingly, the amount of the absorbed water vapor should linearly increase with time. The same point is applied to the finally collected water.

Second, there are relatively large differences among the collected amounts of water on the three types of plates for the cases of 10 and 15 min condensation periods. For example, in the 10 min case, the total amounts of water collected per unit area on the glass, SiO_2, and SU-8 plates were 0.134 ± 0.003, 0.203 ± 0.032, and 0.157 ± 0.030 $\mu L/mm^2$, respectively. The largest difference was ~0.07 $\mu L/mm^2$. After 10 or 15 min condensation, relatively small drops on the SU-8 plates are formed in comparison with those on the other two types of plates (Figure 4d). Consequently, the top SU-8 plate was pressed harder to ensure all the condensed water drops could form bridges, making some drops located near the edge spill out of the plate. In addition, glass plates have relatively high hydrophilicity. Part of the water still sticks to the plate surface after a cycle of squeezing and relaxing processes. Hence, the loss of water during the collection process makes SU-8 and glass plates collect less water.

Third and finally, the differences in the amounts of collected water were smaller in another three cases. After the 30 min condensation, the total amounts of water collected per unit area on the glass, SiO_2, and SU-8 plates did not have much difference, which were 0.55 ± 0.07, 0.52 ± 0.08, and 0.56 ± 0.02 $\mu L/mm^2$, respectively, because the amount of lost water previously mentioned in the second point was much smaller than the total collected water.

Three points were further observed during the squeezing and relaxing processes (Figure 5b–d and the corresponding three videos in Supporting Information). First, water bridges were formed when the top plate was lowered down, even in the 1 min case (Figure 5b2 and Video 1 of Supporting Information). It was found that neighboring water drops were merged to form a large drop, when they elongated and contacted each other due to the pressing of the top plate (Figure 5b3 and Video 1 of Supporting Information). This result implies that the squeezing process actually increased the size of the water drops. Second, during the relaxing process, a water bridge might further merge with its neighboring bridges to form a larger one (Figure 5c3 and d3 and Videos 2 and 3 of Supporting Information). According to the result of ref 35, the shifting distance of a water bridge increases with the drop size. Consequently, due to different shifting distances, a large water bridge may catch up and thus merge with a small bridge in front of it during the relaxing process. The first two points actually aided in the transport of water during a processing cycle. Third, the needed actuation cycles decreased with the increase in the drop sizes. Take the tests on the SiO_2 plates as an example. It took 22 cycles to translate all the drops collected during the 1 min case, 4 cycles for the 5 min period, 1–2 cycles for the 10 min period, but only 1 cycle for both 15 and 30 min cases. As indicated in the first two points, the pressing and relaxing processes resulted in the coalescence of drops. Large drops were formed in the 15 and 30 min cases, and they were merged into a huge one, which was capable of moving to the corner of the two plates during a single actuation cycle (Figure 5d3 and Video 3 of Supporting Information). However, due to relatively small sizes of the condensed drops in another three cases, the merged drops were still not large enough to move to the corner during a single actuation cycle (Figure 5b3 and c3). Thus, in the first three cases, more than 1 actuation cycles were needed to translate all of the collected water to the corner.

4.3. Design and Testing of the Large Collector. As discussed in subsection 4.2, in the 30 min case, the three types of plates collected about the same amount of water, and they all just needed a single actuation cycle to translate all the collected water to the corner. Also, during this actuation process, the condensed drops were all merged together to form a thin film in the squeezing process on each type of plate, making the relaxing degree less than 1° for the whole film to move to the corner. Therefore, we did not see much difference in the fog-collection efficiencies and relaxing angles of the three types of plates.

Next, we compare the plates in the case of collecting a single drop. As shown in Figure 4, the average diameters of condensed drops are 22.7, 15.6, and 8.6 mm at the desired collection times of 20, 28, and 36 min on glass, SiO_2, SU-8 plates, respectively. Accordingly, the drops with the same diameters were placed between the corresponding plates. The break heights of water bridges were measured as 5.1, 6.0, and 5.5 mm, respectively, on glass, SiO_2, and SU-8 plates. Furthermore, when the relaxing angle was 1.2°, the drops began to move toward the corner on each type of plate. According to eq 2, the maximum values of l_1 on the three types of plates did not have a large difference, and they were 24, 29, and 26 cm, respectively.

We then focus on the drop heights on glass, SiO_2, and SU-8 plates at the end of condensation periods, because, as previously discussed in subsection 3.2, these heights affected the values of l_2. After a 36 min condensation period, the heights of drops on glass, SiO_2, and SU-8 plates were measured to be 1.6, 2.5, and 3.2 mm, respectively. Hence, SU-8 plates were chosen for the large collector. These plates were made by coating SU-8 on glass plates. In this collector, l_1 was set to be 26 cm as previously discussed, and l_2 was temporarily chosen to be 10 cm because of the availability of such plates. The thickness of the plates was 0.2 cm.

As shown in Figure 6a, the setup of the large collector is similar to what was illustrated in Figure 2. On the other hand, it has two differences from the one for the small collector (Figure 3): (i) to create a relatively uniform fog environment using our humidifier, instead of an open space, the large collector was placed in a closed glass chamber with dimensions of 40 × 30 × 30 cm^3; and (ii) the mist flow did not directly blow the two plates, and it came in the glass chamber through a top opening.

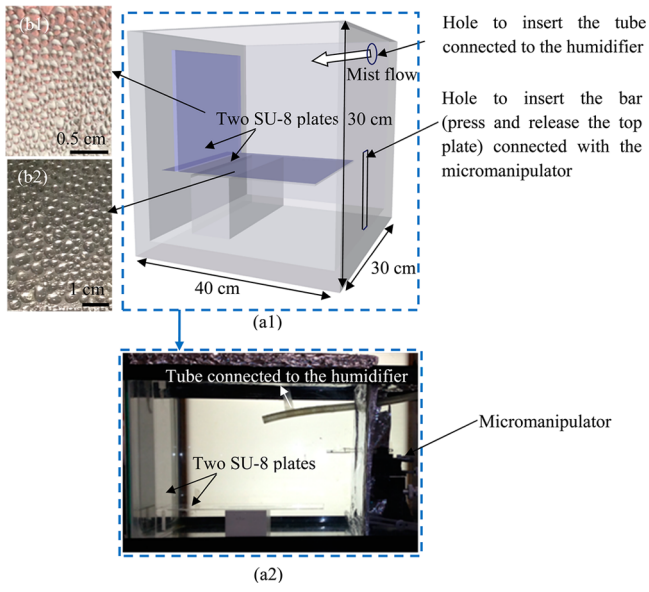

Figure 6. (a) Experimental setup for water collection by two large SU-8 plates with dimensions of 26 × 10 × 0.2 cm^3, and (b) water drops on the surfaces of two plates after 36 min condensation.

As shown in Figure 6b, the average diameters of condensed drops after the 36 min condensation period were about 1 and 5 mm on the surfaces of the top and bottom plates, respectively. During condensation, it was observed that (i) large condensed drops moved down from the top plate to the corner of the two plates due to gravity and (ii) only smaller ones remained on the top plate. Accordingly, the average diameters of condensed drops were different on the surfaces of the two plates. In addition, the average drop sizes on these two plates were smaller than the one in the case of the small collector, which was 8.6 mm. This difference implies that the vapor densities around the two plates of the large collector were lower than that surrounding the bottom plate of the smaller collector, due to the fact that the two plates were not directly blown by the incoming mist flow.

Four tests were done to examine the fog-collection capability of the large collector during a 36 min mist flow. Only 1 cycle of squeezing and relaxing was needed to translate all the condensed drops to the corner of the plates. It took no more than 3 s to complete this cycle, which was much shorter than the condensation period of 36 min. Therefore, although no condensation is performed during the squeezing and relaxing processes, as far as time is concerned, these processes have little influence on water collection. The total amount of collected water was ~15.8 ± 2 mL. The amount of water collected per unit surface area was calculated to be 0.30 μL/mm^2. As expected, this value was less than its counterpart in the case of the small collector, which is ~0.56 μL/mm^2 after 30 min condensation.

As discussed in subsection 3.2, the plate sizes should decrease with the decrease in the humidity level in an environment to effectively transport water drops. In a desert, the fog event normally occurs in the late night and early morning due to relatively low temperature during these periods. It has been reported that, in Chile's desert, the fog can bring in water as much as 1.5 μL/mm^2/h in the morning.[43] This amount is ~2.5 times as much as what has been collected using the large collector during a 1 h period, implying large water drops may still be formed on the plates in this desert. Accordingly, a large collector may be effective as well to collect fog over there.

4.4. Comparison of Fog-Collecting Efficiencies. Fog-collecting efficiencies have been compared in ref 8 among fog-basking beetles, Namib dune bushman grasses, and metal wires. In their case, the temperature was kept between 10 and 15 °C. A humidifier produced 325 mL of fog/h with a speed of 0.1 m/s. All the samples were placed at 23° to the horizontal direction. These samples collected 0.25, 0.48, and 0.61 μL/mm^2, respectively, during the 120 min periods. Our tests on the smaller collector were performed under similar experimental conditions. The condensation and collection were done at room temperature (22 ± 1 °C). The incoming mist flow had an angle of 15° with the bottom plate. It had a speed of 0.08 m/s. The big difference was that the amount of fog produced by our humidifier per hour was 81 mL, which was less than that of ref 8. In the 30 min case of the smaller collector, the average collected water per unit surface area of the bottom SU-8 plate is 0.56 μL/mm^2. When our value is scaled by 4 times from 30 to 120 min (i.e., repeat the 30 min case 3 times), the collected water per unit area is 2.24 μL/mm^2. It is about 9.0, 4.7, and 3.7 times, respectively, as large as the ones of beetles, grasses, and metal wires. It is considered that the active transport of condensed water has the main contribution to the higher collection efficiency of the small collector, which ensured that almost all of the water condensed on the artificial collector was collected. In the cases of fog-basking beetles, Namib dune bushman grasses, and metal wires, as discussed in section 1, the condensed water is translated by gravity and capillary force, which is a passive method and may not be capable of transporting all of the condensed water.

Furthermore, during the 120 min periods, a beetle, a grass, and a metal wire, respectively, collected 0.06, 0.11, and 0.13 mL volumes of water, which are about 33, 18, and 15 times less than what was collected by the small collector if our result is also scaled from 30 to 120 min. Part of the difference is caused by the larger condensation surface area of the small collector. The total surface area of the small collector, which only counts the bottom plate surface, is 882 mm^2. It is larger than the ones reported for individual beetles, grasses, and metal wires,[8] which are 245, 253, and 220 mm^2, respectively. Therefore, in comparison with well-known fog-harvesting animal and plant and an artificial collector, our small collector has demonstrated much higher efficiency in fog collection. This comparison also indicates the importance of both introducing plates (to gain large collection areas) and using the squeezing and relaxing actuation (for actively transporting condensed drops). It is considered that directly testing beetles and grasses in our experimental conditions should give better comparison between them and our collectors. Because of the lack of these desert animals and plants, they are not tested in this work.

Although the amount of water collected by the large collector per unit area is less than the one harvested by the small collector due to different experimental conditions, when our value is scaled from 36 to 120 min, it is still about 3.4, 1.8, and 1.4 times, respectively, as large as the ones of beetles, grasses, and metal wires. In addition, due to its large surface area, which is 52 000 mm^2 and counts the surface areas of both top and bottom plates, the scaled amount of water collected by the large collector is about 878, 479, and 405 times more than what was collected by individual beetles, grasses, or metal wires.

Moreover, vertically oriented plates with hydrophobic or hydrophilic surfaces have been previously tested in refs 18 and 19 for their fog-collecting efficiencies. Due to gravity, large drops that are condensed on a plate can be drained to a container, which is located under the plate. During a 30 min period, the water collected per unit area on a graphene-coated (hydrophobic) surface is 0.148 μL/mm^2,[18] while it is 0.1 μL/mm^2 on a hexamethyldisiloxane (superhydrophilic) surface with the drainage path.[19] These are lower than what has been collected on either our small or large collector. However, due to different experimental conditions, such as humidity and temperature, this comparison is not accurate.

In the cases of refs 18 and 19, tiny drops cannot be drained, because their gravity is less than the resistance force induced by the contact angle hysteresis. Subsequently, not all condensed drops can be collected. Nevertheless, in this work, due to the aid of the squeezing and relaxing processes, such tiny drops can still be collected. Thus, under the same experimental conditions, our collectors should have higher collecting efficiencies when the same plates are used to collect water.

A set of experiments has been done to validate this point. The corresponding experimental setup is similar to the one shown in Figure 6. On the other hand, there are three differences from the tests on the large collector. First, the glass, SiO_2, and SU-8 plates that have been used in the small collectors were adopted in the tests, and in each test only a single plate was put inside the chamber that has a vertical orientation. Second, as in the case of the small collectors, the condensation duration in every test was 30 min, instead of 36 min. Third, the water was collected through two steps instead of a single one. In the first step, water was collected from the bottom of the vertical plate at the end of the condensation period. In the second step, the water that still remained on the vertical plate was collected using the squeezing and relaxing processes, in which the vertical plate served as the top plate while a dry plate functioned as the bottom one.

In our tests, the amounts of water collected from the bottoms of glass, SiO_2, and SU-8 plates at the end of the 30 min condensation period were 0.315, 0.397, and 0.406 μL/mm^2, respectively. After the application of the squeezing and relaxing processes, additional 0.148, 0.072, and 0.075 μL/mm^2 were collected from these plates, separately. These results indicate (i) totally 0.463, 0.470, and 0.482 μL/mm^2 are collected from glass, SiO_2, and SU-8 plates, separately, which also do not vary much with the plates as in the 30 min case of the small collector; (ii) 68%, 85%, and 84% of water drops, which are condensed, respectively, on the three plates, are collected due to gravitational effect; and (iii) the remaining 32%, 15%, and 16%, respectively, of condensed drops can be further collected using the squeezing and relaxing processes. Accordingly, the adoption of the active transportation approach improves the collecting efficiency.

In addition, another two points can be observed from these results. First, the wettability of the surface highly influences the collecting efficiency in the first step, which agrees with what has been observed by other researchers.[18,19] Second, the introduction of squeezing and relaxing actuation ensures that almost all condensed drops can be

collected, which may be a major reason why the three types of plates do not have much difference in the amounts of finally collected water.

5. SUMMARY AND CONCLUSIONS

In this work, motivated by the feeding mechanism of a shorebird, we have developed a plate-based collector to harvest water from fog and dew. As in the case of the shorebird, squeezing and relaxing processes have been applied to facilitate the transport of condensed water drops from the plate surfaces to the corner of two plates. We have explored the condensation and collection of a small version of the artificial collector and found it was much more efficient than desert animal and plants due to the active transport of condensed water, which ensured that almost all of the water condensed on the artificial collector was collected. On the basis of these results, we further developed a large collector. Because of its relatively larger surface areas, 15.8 mL of water was collected during a condensation period of 36 min.

■ ASSOCIATED CONTENT

Supporting Information

Videos of squeezing and relaxing of water drops after mist flows. This material is available free of charge via the Internet at http://pubs.acs.org.

■ AUTHOR INFORMATION

Corresponding Author

*E-mail: chengluo@uta.edu.

Notes

The authors declare no competing financial interest.

■ REFERENCES

(1) Middleton, N. *Deserts: A Very Short Introduction*; Oxford University Press: New York, 2009.
(2) Parker, A. R.; Lawrence, C. R. Water Capture by a Desert Beetle. *Nature* **2001**, *414*, 33−34.
(3) Nørgaard, T.; Dacke, M. Fog-Basking Behaviour and Water Collection Efficiency in Namib Desert Darkling Beetles. *Front. Zool.* **2010**, *7*, 23.
(4) Ju, J.; Bai, H.; Zheng, Y.; Zhao, T.; Fang, R.; Jiang, L. A Multi-structural and Multi-functional Integrated Fog Collection System in Cactus. *Nat. Commun.* **2012**, *3*, 1247.
(5) Heng, X.; Xiang, M.; Lu, Z.; Luo, C. Branched ZnO Wire Structures for Water Collection Inspired by Cacti. *ACS Appl. Mater. Interfaces* **2014**, *6*, 8032−8041.
(6) Andrews, H.; Eccles, E.; Schofield, W.; Badyal, J. Three-Dimensional Hierarchical Structures for Fog Harvesting. *Langmuir* **2011**, *27*, 3798−3802.
(7) Ebner, M.; Miranda, T.; Roth-Nebelsick, A. Efficient Fog Harvesting by *Stipagrostis Sabulicola* (Namib Dune Bushman Grass). *J. Arid Environ.* **2011**, *75*, 524−531.
(8) Nørgaard, T.; Ebner, M.; Dacke, M. Animal or Plant: Which is the Better Fog Water Collector? *PLoS One* **2012**, *7*, e34603.
(9) Lorenceau, É.; Quéré, D. Drops on a Conical Wire. *J. Fluid Mech.* **2004**, *510*, 29−45.
(10) Zheng, Y.; Bai, H.; Huang, Z.; Tian, X.; Nie, F.-Q.; Zhao, Y.; Zhai, J.; Jiang, L. Directional Water Collection on Wetted Spider Silk. *Nature* **2010**, *463*, 640−643.
(11) Zhai, L.; Berg, M. C.; Cebeci, F. C.; Kim, Y.; Milwid, J. M.; Rubner, M. F.; Cohen, R. E. Patterned Superhydrophobic Surfaces: Toward a Synthetic Mimic of the Namib Desert Beetle. *Nano Lett.* **2006**, *6*, 1213−1217.
(12) Garrod, R.; Harris, L.; Schofield, W.; McGettrick, J.; Ward, L.; Teare, D.; Badyal, J. Mimicking a Stenocara Beetle's Back for Microcondensation Using Plasmachemical Patterned Superhydrophobic−Superhydrophilic Surfaces. *Langmuir* **2007**, *23*, 689−693.
(13) Dorrer, C.; Rühe, J. R. Mimicking the Stenocara Beetle Dewetting of Drops from a Patterned Superhydrophobic Surface. *Langmuir* **2008**, *24*, 6154−6158.
(14) Thickett, S. C.; Neto, C.; Harris, A. T. Biomimetic Surface Coatings for Atmospheric Water Capture Prepared by Dewetting of Polymer Films. *Adv. Mater.* **2011**, *23*, 3718−3722.
(15) Ozden, S.; Ge, L.; Narayanan, T. N.; Hart, A. H. C.; Yang, H.; Sridhar, S.; Vajtai, R.; Ajayan, P. M. Anisotropically Functionalized Carbon Nanotube Array Based Hygroscopic Scaffolds. *ACS Appl. Mater. Interfaces* **2014**, *6*, 10608−10613.
(16) Ju, J.; Xiao, K.; Yao, X.; Bai, H.; Jiang, L. Bioinspired Conical Copper Wire with Gradient Wettability for Continuous and Efficient Fog Collection. *Adv. Mater.* **2013**, *25*, 5937−5942.
(17) Domen, J. K.; Stringfellow, W. T.; Camarillo, M. K.; Gulati, S. Fog Water as an Alternative and Sustainable Water Resource. *Clean Technol. Environ. Policy* **2014**, *16*, 235−249.
(18) Kim, G.-T.; Gim, S.-J.; Cho, S.-M.; Koratkar, N.; Oh, I.-K. Wetting-Transparent Graphene Films for Hydrophobic Water-Harvesting Surfaces. *Adv. Mater.* **2014**, *26*, 5166−5172.
(19) Lee, A.; Moon, M.-W.; Lim, H.; Kim, W.-D.; Kim, H.-Y. Water Harvest via Dewing. *Langmuir* **2012**, *28*, 10183−10191.
(20) Conley, J., Jr; Stecker, L.; Ono, Y. Directed Assembly of ZnO Nanowires on a Si Substrate without a Metal Catalyst Using a Patterned ZnO Seed Layer. *Nanotechnology* **2005**, *16*, 292−296.
(21) Chakraborty, A.; Liu, X.; Wang, H.; Luo, C. Generation of ZnO Nanowires with Varied Densities and Lengths by Tilting a Substrate. *Microsyst. Technol.* **2012**, *18*, 1497−1506.
(22) Dalal, S.; Baptista, D.; Teo, K.; Lacerda, R.; Jefferson, D.; Milne, W. Controllable Growth of Vertically Aligned Zinc Oxide Nanowires Using Vapour Deposition. *Nanotechnology* **2006**, *17*, 4811−4818.
(23) Huang, M. H.; Wu, Y.; Feick, H.; Tran, N.; Weber, E.; Yang, P. Catalytic Growth of Zinc Oxide Nanowires by Vapor Transport. *Adv. Mater.* **2001**, *13*, 113−116.
(24) Greene, L. E.; Law, M.; Tan, D. H.; Montano, M.; Goldberger, J.; Somorjai, G.; Yang, P. General Route to Vertical ZnO Nanowire Arrays Using Textured ZnO Seeds. *Nano Lett.* **2005**, *5*, 1231−1236.
(25) Hsu, J. W.; Tian, Z. R.; Simmons, N. C.; Matzke, C. M.; Voigt, J. A.; Liu, J. Directed Spatial Organization of Zinc Oxide Nanorods. *Nano Lett.* **2005**, *5*, 83−86.
(26) Cheng, C.; Fan, H. J. Branched Nanowires: Synthesis and Energy Applications. *Nano Today* **2012**, *7*, 327−343.
(27) Bierman, M. J.; Jin, S. Potential Applications of Hierarchical Branching Nanowires in Solar Energy Conversion. *Energy Environ. Sci.* **2009**, *2*, 1050−1059.
(28) Cao, M.; Ju, J.; Li, K.; Dou, S.; Liu, K.; Jiang, L. Facile and Large-Scale Fabrication of a Cactus-Inspired Continuous Fog Collector. *Adv. Funct. Mater.* **2014**, *24*, 3235−3240.
(29) Zweers, G. Transformation of Avian Feeding Mechanisms: A Deductive Method. *Acta Biotheor.* **1991**, *39*, 15−36.
(30) Rubega, M. A.; Obst, B. S. Surface-Tension Feeding in Phalaropes: Discovery of a Novel Feeding Mechanism. *Auk* **1993**, *110*, 169−178.
(31) Rubega, M. A. Surface Tension Prey Transport in Shorebirds: How Widespread Is It? *Ibis* **1997**, *139*, 488−493.
(32) Estrella, S. M.; Masero, J. A.; Pérez-Hurtado, A.; Hepp, G. Small-Prey Profitability: Field Analysis of Shorebirds' Use of Surface Tension of Water to Transport Prey. *Auk* **2007**, *124*, 1244−1253.
(33) Prakash, M.; Quéré, D.; Bush, J. W. Surface Tension Transport of Prey by Feeding Shorebirds: The Capillary Ratchet. *Science* **2008**, *320*, 931−934.
(34) Bush, J. W.; Peaudecerf, F.; Prakash, M.; Quéré, D. On a Tweezer for Droplets. *Adv. Colloid Interface Sci.* **2010**, *161*, 10−14.
(35) Luo, C.; Heng, X.; Xiang, M. Behavior of a Liquid Drop Between Two Nonparallel Plates. *Langmuir* **2014**, *30*, 8373−8380.
(36) Lafuma, A.; Quéré, D. Superhydrophobic States. *Nat. Mater.* **2003**, *2*, 457−460.

(37) Xiang, M.; Wilhelm, A.; Luo, C. Existence and Role of Large Micropillars on the Leaf Surfaces of *The President* Lotus. *Langmuir* **2013**, *29*, 7715−7725.
(38) Luo, C.; Xiang, M. Wetting States on Circular Micropillars with Convex Sidewalls after Liquids Contact Groove Base. *Langmuir* **2013**, *29*, 15065−15075.
(39) Luo, C.; Xiang, M. Existence and Stability of an Intermediate Wetting State on Circular Micropillars. *Microfluid. Nanofluid.* **2014**, *17*, 539−548.
(40) De Gennes, P.-G.; Brochard-Wyart, F.; Quéré, D. *Capillarity and Wetting Phenomena: Drops, Bubbles, Pearls, Waves*; Springer: Berlin, 2003.
(41) Viovy, J. L.; Beysens, D.; Knobler, C. M. Scaling Description for the Growth of Condensation Patterns on Surfaces. *Phys. Rev. A* **1988**, *37*, 4965.
(42) Narhe, R.; Beysens, D. Nucleation and Growth on a Superhydrophobic Grooved Surface. *Phys. Rev. Lett.* **2004**, *93*, 076103.
(43) Schemenauer, R. S.; Cereceda, P. A Proposed Standard Fog Collector for Use in High-Elevation Regions. *J. Appl. Meteorol.* **1994**, *33*, 1313−1322.